Fluctuations of Bacteriochlorophyll's Positions in B850 Ring from Photosynthetic Complex LH2

Pavel Heřman, David Zapletal

***Abstract*—** Interactions with environment have large impact on the properties of light–harvesting (LH) pigment–protein complexes. Some of these interactions could be modeled by different types of static disorder. Fluctuations of bacteriochlorophyll's positions in B850 ring from LH2 complex of purple bacteria are investigated in present paper. The nearest neighbour approximation model of the ring is considered. Four modifications of such uncorrelated Gaussian static disorder type (fluctuations of radial positions of molecules on the ring, fluctuations of angular positions of molecules on the ring, fluctuations of molecular positions in perpendicular direction to the ring plane and fluctuations of molecular positions in arbitrary direction) are taking into account. The most important statistical properties of the nearest neighbour transfer integral distributions for different strengths of static disorder are calculated, discussed and compared.

***Keywords*—**LH2 complex, B850 ring, static disorder, Hamiltonian, transfer integral distributions

I. Introduction

GREEN plants and certain other organisms (bacteria, blue–green algae) are able to transform light energy into chemical energy in the process which is called photosynthesis. Light energy is captured during this process and used for conversion of water, carbon dioxide and minerals into energy–rich organic compounds and (in most cases) oxygen. The process of photosynthesis occurs in two stages. Photochemical reactions (i.e., light–capture) take place in the first (light) stage. During this first stage, light is absorbed and used for driving a series of electron transfers. They result in synthesis of ATP and reduced form of nicotine adenine dinucleotide phosphate (NADPH). Second (dark) stage comprises chemical reactions controlled by enzymes. The ATP and NADPH formed in the light–capturing reactions are used to reduce carbon dioxide to organic carbon compounds [1].

Investigation of photosynthesis has been in the focus of researchers for a long time. Our interest is mainly focused on first (light) stage of photosynthesis in purple bacteria. A complex system of membrane–associated pigment–proteins (light–harvesting (LH) antenna) absorbs solar photons. Excitation energy (in the form of Frenkel exciton) is very efficiently transferred to a reaction center, where conversion of the light energy into a chemical energy occurs [2]. The antenna systems of photosynthetic complexes from purple bacteria are formed by ring units LH1, LH2, LH3, and LH4. Their geometric structures are known in great detail from X–ray crystallography. All these light–harvesting complexes have generally the same organization: cyclic repetition of identical subunits in such a way that a ring–shaped structure is formed. However the symmetries of these rings are different.

The first description of crystal structure of LH2 complex contained in purple bacterium *Rhodopseudomonas acidophila* in high resolution was given by McDermott et al. [3], then further e.g. by Papiz et al. [4]. The bacteriochlorophyll (BChl) molecules are organized in two concentric rings. One ring (B850 ring) is composed of eighteen closely packed BChl molecules with absorption band at about 850 nm. Second ring (B800 ring) consists of nine well–separated BChl molecules (B800) absorbing around 800 nm. Dipole moments of BChl molecules in LH2 complex have approximately tangential arrangement. The whole LH2 complex consists of nine identical subunits, it is nonameric. LH2 complexes from other purple bacteria have analogous ring structure.

Other types of light–harvesting complexes such as the B800–820 LH3 complex or LH4 complex can be also found in some bacteria (LH3 in *Rhodopseudomonas acidophila* strain 7050, LH4 in *Rhodopseudomonas palustris*). They can differ in number of BChl molecules – LH3 complex like LH2 one is usually nonameric but LH4 complex is octameric (it consists of eight identical subunits). They have also different orientations of molecular dipole moments. Therefore strengths of mutual interactions between bacteriochorophylls are different too. For instance, dipole moments of BChl molecules in B–α/B–β ring from LH4 complex are oriented approximately radially to the ring. Interactions between the

Manuscript received November, 2016.

This work was supported by the Faculty of Science, University of Hradec Králové (project of specific research No. 2105/2016 – P. Heřman).

P. Heřman is with the Department of Physics, Faculty of Science, University of Hradec Králové, Rokitanského 62, 50003 Hradec Králové, Czech Republic (e-mail: pavel.herman@uhk.cz).

D. Zapletal is with the Institute of Mathematics and Quantitative Methods, Faculty of Economics and Administration, University of Pardubice, Studentská 95, 53210 Pardubice, Czech Republic (e-mail: david.zapletal@upce.cz).

nearest neighbour bacteriochlorophylls in B–α/B–β ring are approximately two times weaker in comparison with B850 ring from LH2 complex and they have opposite sign. LH4 complex also contains another BChl ring, i.e. it consists of three Bchl rings [5].

The intermolecular distances under 1 nm determine strong exciton couplings between corresponding pigments. Therefore an extended Frenkel exciton states model could be used in theoretical approach. At room temperature the solvent and protein environment fluctuates with characteristic time scales ranging from femtoseconds to nanoseconds. Fast fluctuations can be modeled by dynamic disorder and slow fluctuations by static disorder. Kumble and Hochstrasser [6] and Nagarajan et al. [7], [8] studied static disorder effect on the anisotropy of fluorescence for LH2 complexes. We extended these investigations by consideration of dynamic disorder. This effect was studied by us for simple model systems [9]–[11] and then for models of B850 ring (from LH2) [12], [13]. Various types of uncorrelated static disorder (in local excitation energies, in transfer integrals, etc.) and correlated one (e.g., elliptical deformation) were used in the past [14]–[16] and also different arrangements of optical dipole moments were compared [17]–[20]. Recently we have focused on the modeling of absorption and steady state fluorescence spectra of LH2 and LH4 complexes within the nearest neighbour approximation model [21]–[25]. We have also extended our model to full Hamiltonian model and published the results for different types of static disorder [26]–[34].

Main goal of the present paper is the investigation of the nearest neighbour transfer integral distributions for various types of static disorder and comparison of their influence on Hamiltonian of B850 ring from LH2 complex. The rest of the paper is structured as follows. Section II introduces the ring model with different types and modifications of static disorder. Used units and parameters could be found in Section III. Results are presented and discussed in Section IV and some conclusions are drawn in Section V.

II. Model

The Hamiltonian of an exciton on molecular ring, e.g. B850 ring from LH2 complex, reads

$$H = H^0_{\rm ex} + H_{\rm s} + H_{\rm ph} + H_{\rm ex-ph}. \qquad (1)$$

The first term, $H^0_{\rm ex}$, describes an exciton on the ideal ring, i.e. without any disorder. The second term, $H_{\rm s}$, corresponds to static disorder and the third and fourth terms, $H_{\rm ph}$ and $H_{\rm ex-ph}$, represents dynamic disorder, i.e. phonon bath and exciton–phonon interaction. We consider only static disorder in this paper.

A. Ideal ring

Hamiltonian of an exciton on the ideal ring reads

$$H^0_{\rm ex} = \sum_{m=1}^{N} E^0_m a^\dagger_m a_m + \sum_{m,n=1(m\neq n)}^{N} J^0_{mn} a^\dagger_m a_n. \qquad (2)$$

$a^\dagger_m$ (a_m) are creation (annihilation) operators of an exciton at site m, E^0_m is the local excitation energy of m–th molecule, J^0_{mn} (for $m \neq n$) is the so–called transfer integral between sites m and n. N is the number of molecules in the ring ($N = 18$ for B850 ring form LH2 complex). Local excitation energies E^0_m are the same for all bacteriochlorophylls on unperturbed ring, i.e.

$$E^0_m = E_0, \quad m = 1, \ldots, N.$$

The interaction strengths between the nearest neighbour bacteriochlorophylls inside one subunit and between subunits are almost the same in B850 ring from LH2 complex (see Figure 1 (B) in [5]). That is why such ring can be modeled as homogeneous case,

$$J^0_{mn} = J^0_{m+i,n+i}. \qquad (3)$$

In dipole–dipole approximation, transfer integrals J_{mn} can be written as

$$J_{mn} = \frac{\vec{d}_m \cdot \vec{d}_n}{|\vec{r}_{mn}|^3} - 3\frac{\left(\vec{d}_m \cdot \vec{r}_{mn}\right)\left(\vec{d}_n \cdot \vec{r}_{mn}\right)}{|\vec{r}_{mn}|^5} = \\ = |\vec{d}_m||\vec{d}_n|\frac{\cos\varphi_{mn} - 3\cos\varphi_m \cos\varphi_n}{|\vec{r}_{mn}|^3}. \qquad (4)$$

Here $\vec{d}_m$ and $\vec{d}_n$ are local dipole moments of m–th and n–th molecule respectively, $\vec{r}_{mn}$ is the vector connecting m–th and n–th molecule and φ_m (φ_n) is the angle between $\vec{d}_m$ ($\vec{d}_n$) and $\vec{r}_{mn}$. The angle between m–th and n–th vector of local dipole moment ($\vec{d}_m$, $\vec{d}_n$) is referred to as φ_{mn}. Geometric arrangement of the ring has to correspond with the interaction strengths between the nearest neighbour bacteriochlorophylls. That is why distances $r_{m,m+1}$ of neighbouring molecules in B850 ring from the LH2 complex have to be the same (without any disorder) and angles $\beta_{m,m+1}$ have to be the same too ($\beta_{m,m+1} = 2\pi/18$, see Figure 1).

In what follows we consider the nearest neighbour approximation model, i.e. only the nearest neighbour transfer matrix elements are nonzero. In this case we have

$$J^0_{mn} = J_0(\delta_{m,n+1} + \delta_{m,n-1}). \qquad (5)$$

The pure exciton Hamiltonian $H^0_{\rm ex}$ can be diagonalized using the wave vector representation with corresponding delocalized Bloch states α and energies E_α. Using Fourier transformed excitonic operators a_α, the Hamiltonian in α–representation reads

$$H^0_{\rm ex} = \sum_{\alpha=1}^{N} E_\alpha a^\dagger_\alpha a_\alpha. \qquad (6)$$

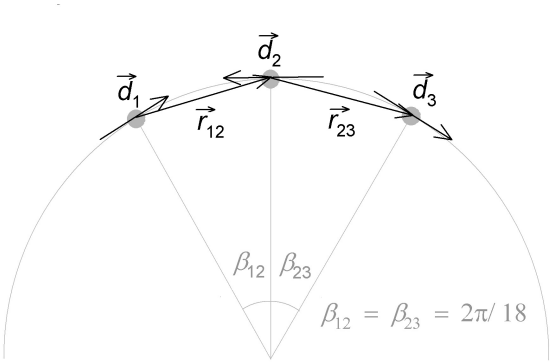

Fig. 1. Geometric arrangement of ideal B850 ring from LH2 complex (without any fluctuations)

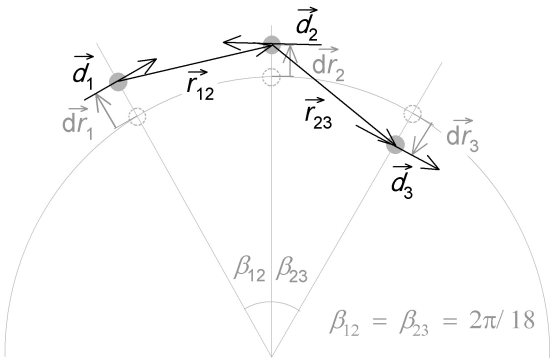

Fig. 2. B850 ring from LH2 complex – fluctuations in radial positions of bacteriochlorophylls δr_m

The form of operators a_α is

$$a_\alpha = \sum_{n=1}^{N} a_n \mathrm{e}^{\mathrm{i}\alpha n},\ \alpha = \frac{2\pi}{N} l,\ l = 0, \ldots, \pm\frac{N}{2}, \quad (7)$$

and the simplest exciton Hamiltonian for B850 ring from LH2 complex in α–representation is given by Eq. (6) with

$$E_\alpha = E_0 - 2J_0 \cos\alpha. \quad (8)$$

B. Static disorder

As concerns static disorder (second term in Eq. (1)), we can model it as fluctuations in local excitation energies of bacteriochlorophylls $\delta\varepsilon_m$,

$$E_m = E_0 + \delta\varepsilon_m, \quad (9)$$

or fluctuations in transfer integrals δJ_{mn} $(m \neq n)$,

$$J_{mn} = J_{nm} = J^0_{mn} + \delta J_{mn}. \quad (10)$$

δJ_{mn} can be treated as uncorrelated Gaussian fluctuations (with the standard deviation Δ_J). Better way for modeling of δJ_{mn} is to connect these fluctuations with disorder in geometric arrangement of the ring. Deviations of ring geometry can be consider in two ways – fluctuations in molecular positions or fluctuations in molecular dipole moment orientations. In the present paper we investigate only the first one, i.e. deviations of molecular positions.

If the positions of molecules are changed in the plane of the ideal ring, than following types of geometric deviations can be considered:

a) uncorrelated fluctuations of radial positions of molecules δr_m on the ring (Gaussian distribution and standard deviation Δ_r),

$$r_m = r_0 + \delta r_m, \quad (11)$$

where r_0 is the radius of the ideal ring without any disorder (see Figure 2);

b) uncorrelated fluctuations of angular positions of molecules $\delta\nu_m$ on the ring (Gaussian distribution and standard deviation Δ_ν),

$$\nu_m = \nu^0_m + \delta\nu_m, \quad (12)$$

where ν^0_m is the angular position of m–th bacteriochlorophyll on the ring, directions of bacteriochlorophyll dipole moments in new positions are unchanged (see Figure 3).

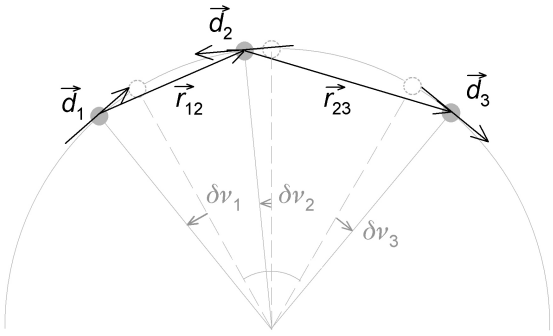

Fig. 3. B850 ring from LH2 complex – fluctuations in angular positions of bacteriochlorophylls $\delta\nu_m$

If the positions of molecules are changed out of the plane of ideal ring we have:

c) uncorrelated fluctuations of molecular positions δz_m – fluctuations occur only in perpendicular direction to the ring plane (Gaussian distribution and standard deviation Δ_z),

$$z_m = \delta z_m. \quad (13)$$

Here z_m determines the distance of m–th bacteriochlorophyll molecule from the plane of ideal ring.

Previous three types are included in more general type of geometric disorder:

d) uncorrelated fluctuations of molecular positions in arbitrary direction $\delta\vec{r}_m$,

$$\vec{r}_m = \vec{r}^{\,0}_m + \delta\vec{r}_m.$$

Here $\vec{r}_m$ denotes position vector of m–th molecule and $\vec{r}_m^{\,0}$ is position vector of m–th molecule on unperturbed ring. The distributions of molecular distances from positions on unperturbed ring are supposed to be uncorrelated with Gaussian distribution and standard deviation Δ_ρ and distributions in directions of molecular shifts are supposed to be uncorrelated and uniform.

Due to the consideration of dipole–dipole approximation the connection between disorder in geometric arrangement and in transfer integrals is given by Eq. (4).

III. Units and Parameters

Dimensionless energies normalized to the transfer integral $J_{m,m+1} = J_0$ (see Eq. (5)) have been used in our calculations. Estimation of J_0 varies in literature between 250 cm^{-1} and 400 cm^{-1}.

In our previous investigations [35] we found from comparison with experimental results for B850 ring from the LH2 complex [36] that the possible strength Δ_J of the uncorrelated Gaussian static disorder in transfer integrals δJ_{mn} is approximately $\Delta_J \approx 0.15\ J_0$. The strengths of above mentioned types of static disorder in ring geometry is taken in connection with the strength Δ_J. That is why for our types of static disorder we have taken the strengths in following intervals:

a) uncorrelated fluctuations of radial positions of molecules δr_m

$$\Delta_r \in \langle 0.02\ r_0, 0.30\ r_0 \rangle,$$

b) uncorrelated fluctuations of angular positions of molecules $\delta \nu_m$

$$\Delta_\nu \in \langle 0.001\ \pi, 0.022\ \pi \rangle,$$

c) uncorrelated fluctuations of molecular positions δz_m – fluctuations occur only in perpendicular direction to the ring plane

$$\Delta_z \in \langle 0.02\ r_0, 0.30\ r_0 \rangle,$$

d) uncorrelated fluctuations of molecular positions in arbitrary direction $\delta \vec{r}_m$

$$\Delta_\rho \in \langle 0.02\ r_0, 0.30\ r_0 \rangle.$$

In all cases calculations were done for 10000 realizations of static disorder.

IV. Results and Discussion

Various types of static disorder connected with fluctuations in ring geometry and their influence on Hamiltonian of B850 ring from LH2 complex (namely on the nearest neighbour transfer integrals) are investigated in present paper. Distributions of the nearest neighbour transfer integrals $J_{m,m+1}$ were calculated for above mentioned four modifications of static disorder. These distributions are graphically presented by contour plots and also by line plots. Contour plots also contain values of $E(J_{m,m+1})$ and $E(J_{m,m+1}) \pm \sqrt{D(J_{m,m+1})}$. Here $E(J_{m,m+1})$ is sample expected value,

$$E(J_{m,m+1}) = \frac{1}{n} \sum_{i=1}^{n} J_{m,m+1}, \tag{14}$$

and $\sqrt{D(J_{m,m+1})}$ is sample standard deviation,

$$\sqrt{D(J_{m,m+1})} = \sqrt{\frac{1}{(n-1)} M_2}. \tag{15}$$

Additionally, we calculated sample skewness α_3,

$$\alpha_3 = \frac{n^{\frac{5}{2}}}{(n-1)(n-2)} \frac{M_3}{M_2^{\frac{3}{2}}}, \tag{16}$$

and sample kurtosis α_4,

$$\alpha_4 = \frac{n^2}{(n-2)(n-3)} \left[\frac{n(n+1)}{n-1} \frac{M_4}{M_2^2} - 3 \right]. \tag{17}$$

Here

$$M_k = \sum_{i=1}^{n} \left[J_{m,m+1} - E(J_{m,m+1}) \right]^k \tag{18}$$

and n is the number of cases in our samples ($n = 180000$). It corresponds with dimension of Hamiltonian ($N = 18$) and number of static disorder realizations (10000). For more detailed comparison of different static disorder modifications also sample coefficient of variation c was calculated,

$$c = \sqrt{D(J_{m,m+1})} / E(J_{m,m+1}). \tag{19}$$

Distributions of the nearest neighbour transfer integrals $J_{m,m+1}$ for above mentioned types of static disorder are presented in Figure 4 – Figure 7. Figure 4 shows the distributions of $J_{m,m+1}$ for Gaussian uncorrelated static disorder δr_m in radial positions of molecules on the ring. The distributions of $J_{m,m+1}$ for other three above mentioned types of static disorder can be seen in Figure 5 (Gaussian uncorrelated fluctuations of angular positions of molecules on the ring $\delta \nu_m$), in Figure 6 (uncorrelated fluctuations of molecular positions δz_m) and in Figure 7 (uncorrelated fluctuations of molecular positions $\delta \vec{r}_m$ in arbitrary direction). For static disorder in ring geometry expected value $E(J_{m,m+1})$ depends on static disorder strength. Dependencies of $E(J_{m,m+1})$ and $\sqrt{D(J_{m,m+1})}$ on corresponding static disorder strength are also presented in Figure 4 – left column (δr_m), Figure 5 – left column ($\delta \nu_m$), Figure 6 – left column (δz_m) and Figure 7 – left column ($\vec{r}_m$). Values of $E(J_{m,m+1})$, $\sqrt{D(J_{m,m+1})}$, α_3, α_4 and c (see Eq. (14) – Eq. (19)) for chosen static

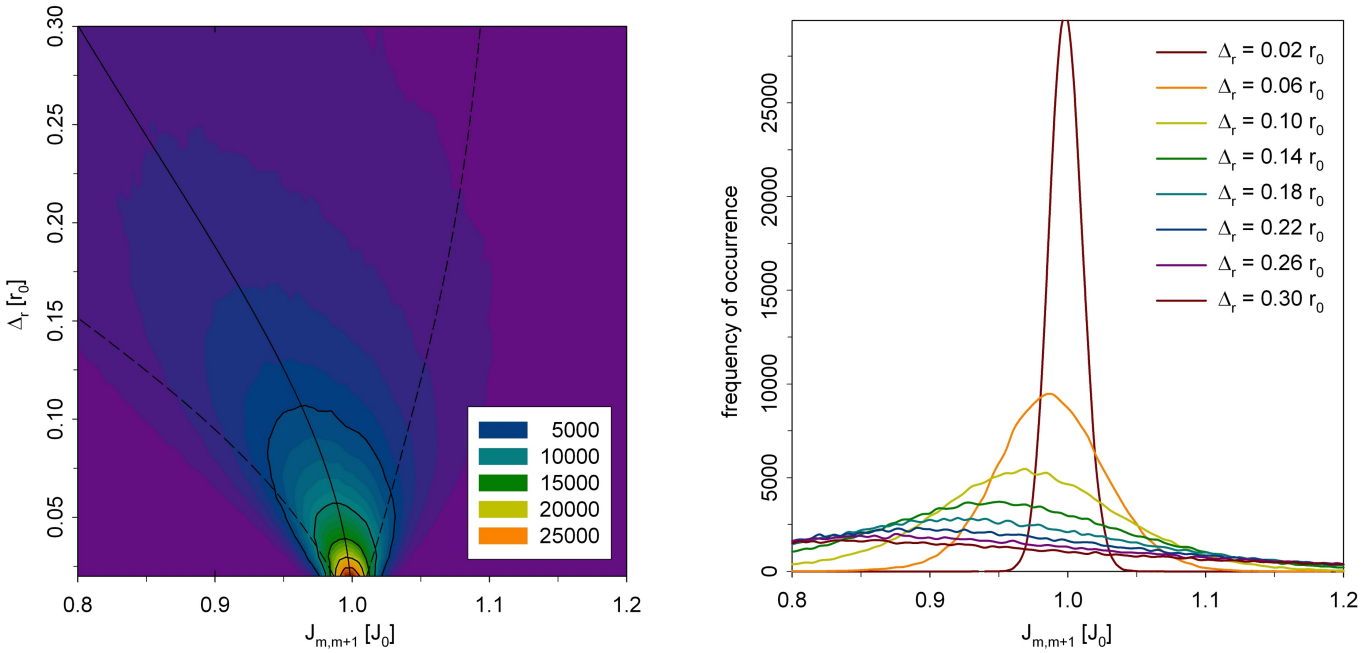

Fig. 4. Distributions of the nearest neighbour transfer integrals $J_{m,m+1}$ for B850 ring from LH2 complex – uncorrelated fluctuations δr_m in radial positions of molecules on the ring (Gaussian distribution and standard deviation Δ_r, strengths of static disorder $\Delta_r \in \langle 0.02\ r_0, 0.30\ r_0 \rangle$)

Δ_r	expected value $E(J_{m,m+1})$	standard deviation $\sqrt{D(J_{m,m+1})}$	skewness α_3	kurtosis α_4	coefficient of variation c
0.02 r_0	0.999 J_0	0.012 J_0	0.083	0.030	0.012
0.06 r_0	0.988 J_0	0.040 J_0	-0.034	0.506	0.040
0.10 r_0	0.967 J_0	0.075 J_0	-0.309	1.230	0.078
0.14 r_0	0.939 J_0	0.118 J_0	-0.447	1.446	0.125
0.18 r_0	0.907 J_0	0.163 J_0	-0.434	1.277	0.179
0.22 r_0	0.872 J_0	0.208 J_0	-0.327	1.031	0.238
0.26 r_0	0.836 J_0	0.252 J_0	-0.165	0.890	0.301
0.30 r_0	0.800 J_0	0.293 J_0	0.024	0.903	0.366

TABLE I
EXPECTED VALUE, STANDARD DEVIATION, SKEWNESS, KURTOSIS AND COEFFICIENT OF VARIATION FOR THE NEAREST NEIGHBOUR TRANSFER INTEGRAL $J_{m,m+1}$ DISTRIBUTIONS OF UNCORRELATED GAUSSIAN FLUCTUATIONS δr_m IN RADIAL POSITIONS OF MOLECULES ON THE RING (EIGHT STRENGTHS Δ_r)

disorder strengths are presented in Table I (δr_m), Table II ($\delta \nu_m$), Table III (δz_m) and Table IV ($\delta \vec{r}_m$).

In case of Gaussian distribution of transfer integrals $J_{m,m+1}$ expected value $E(J_{m,m+1})$ is independent of static disorder strength ($E(J_{m,m+1}) = J_0$) and standard deviation $\sqrt{D(J_{m,m+1})}$ equals the strength of static disorder $\sqrt{D(J_{m,m+1})} = \Delta_J$. That is why, coefficient of variation c corresponds to relative strength of static disorder, i.e. $c = \Delta_J / J_0$ (see Eq. (19)). In this case skewness α_3 and kurtosis α_4 equal zero, i.e. they are also independent of static disorder strength Δ_J.

At the present paper we consider only types of static disorder connected with deviations in positions of molecules (δr_m, $\delta \nu_m$, δz_m and $\delta \vec{r}_m$). In all these cases Gaussian distribution of molecular positions results in non–Gaussian distribution of transfer integrals $J_{m,m+1}$. Therefore expected value $E(J_{m,m+1})$, skewness α_3 and kurtosis α_4 are nonconstant and standard deviation $\sqrt{D(J_{m,m+1})}$ does not equal the strength of static disorder (see Figures 4 – 7 and Tables I – IV). As concerns expected value $E(J_{m,m+1})$, we can see increase of it for increasing static disorder strength in case of fluctuations $\delta \nu_m$ in angular positions of molecules on the ring (see Figure 5 and Table II). On the other hand, $E(J_{m,m+1})$ decreases with growing strength of static

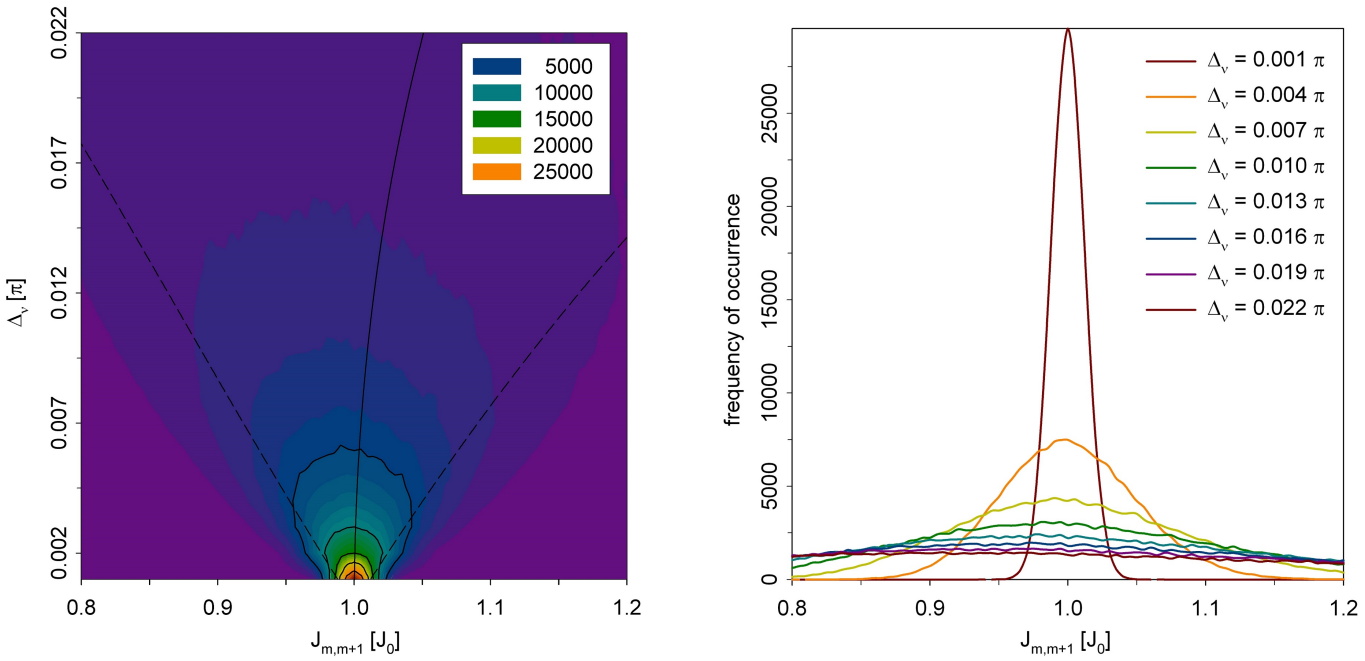

Fig. 5. Distributions of the nearest neighbour transfer integrals $J_{m,m+1}$ for B850 ring from LH2 complex – uncorrelated fluctuations $\delta\nu_m$ in angular positions of molecules on the ring (Gaussian distribution and standard deviation Δ_ν, strengths of static disorder $\Delta_\nu \in \langle 0.001\ \pi, 0.022\ \pi\rangle$)

Δ_ν	expected value $E(J_{m,m+1})$	standard deviation $\sqrt{D(J_{m,m+1})}$	skewness α_3	kurtosis α_4	coefficient of variation c
0.001 π	1.000 J_0	0.012 J_0	0.042	0.004	0.012
0.004 π	1.002 J_0	0.049 J_0	0.189	0.065	0.049
0.007 π	1.005 J_0	0.086 J_0	0.339	0.211	0.086
0.010 π	1.010 J_0	0.124 J_0	0.494	0.455	0.123
0.013 π	1.017 J_0	0.164 J_0	0.657	0.815	0.162
0.016 π	1.026 J_0	0.206 J_0	0.834	1.327	0.201
0.019 π	1.037 J_0	0.251 J_0	1.018	1.959	0.242
0.022π	1.050 J_0	0.298 J_0	1.164	2.348	0.284

TABLE II
EXPECTED VALUE, STANDARD DEVIATION, SKEWNESS, KURTOSIS AND COEFFICIENT OF VARIATION FOR THE NEAREST NEIGHBOUR TRANSFER INTEGRAL $J_{m,m+1}$ DISTRIBUTIONS OF UNCORRELATED GAUSSIAN FLUCTUATIONS $\delta\nu_m$ IN ANGULAR POSITIONS OF MOLECULES ON THE RING (EIGHT STRENGTHS Δ_ν)

disorder in all other types of fluctuations (δr_m – see Figure 4 and Table I, δz_m – see Figure 6 and Table III and $\delta\vec{r}_m$ – see Figure 7 and Table IV). The most important change of expected value occurs in case of fluctuations δr_m in radial positions of molecules and fluctuations δz_m of molecular positions in perpendicular direction to the ring plane. In contrast with these types of static disorder the changes of $E(J_{m,m+1})$ are low for fluctuations $\delta\nu_m$ in angular positions of molecules and fluctuations $\delta\vec{r}_m$ of molecular positions in arbitrary direction.

In all four types of static disorder dependence of standard deviation $\sqrt{D(J_{m,m+1})}$ on static disorder strength is nonlinear. The value of standard deviation does not exceed 0.3 J_0 for static disorder types a), b) and c) (δr_m, $\delta\nu_m$ and δz_m) for the highest strength of corresponding static disorder. On the other hand, in case of static disorder type d) ($\delta\vec{r}_m$) standard deviation grows up much more and its value almost approaches the value of the nearest neighbour transfer integral in the ideal ring, i.e. $\sqrt{D(J_{m,m+1})} \approx 1.0\ J_0$. This leads us to the conclusion that the strengths $\Delta_\rho > 0.15\ r_0$ are unrealistic for this type of static disorder. Such strengths Δ_ρ give also disproportionately high values of skewness and kurtosis (see Table IV).

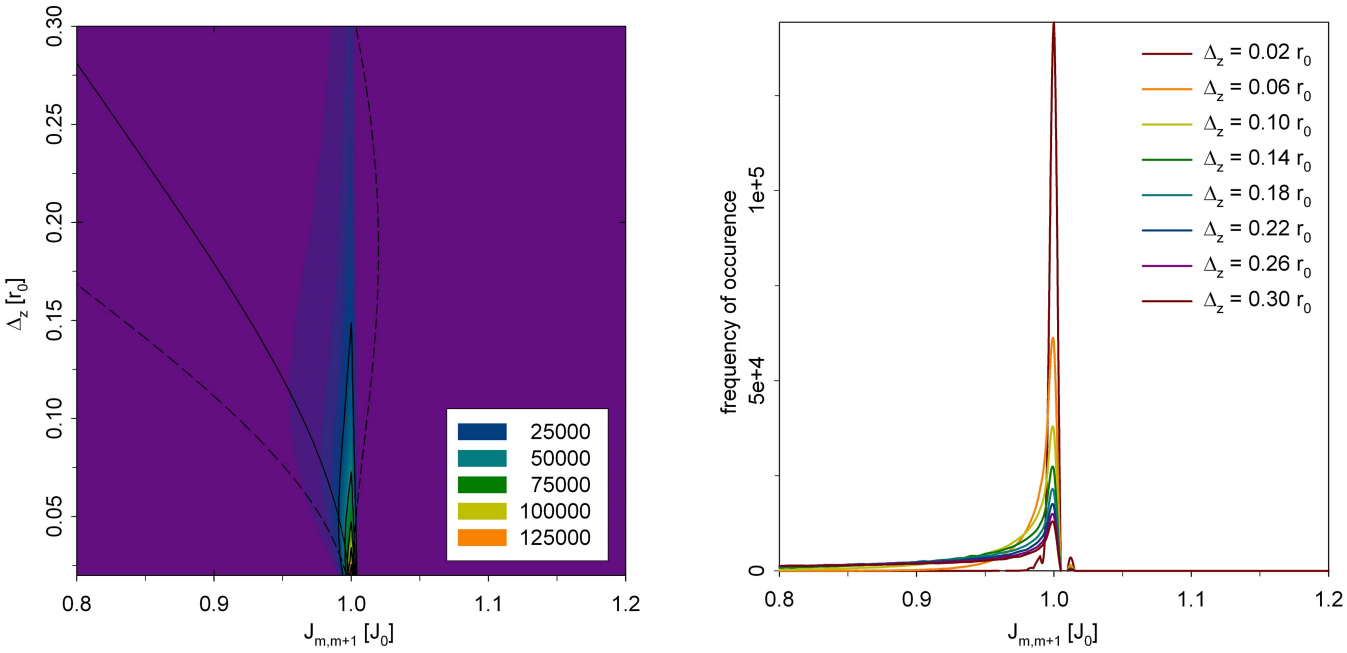

Fig. 6. Distributions of the nearest neighbour transfer integrals $J_{m,m+1}$ for B850 ring from LH2 complex – uncorrelated fluctuations δz_m in molecular positions – fluctuations occur only in perpendicular direction to the ring plane (Gaussian distribution and standard deviation Δ_z, strengths of static disorder $\Delta_z \in \langle 0.02\ r_0, 0.30\ r_0 \rangle$)

Δ_z	expected value $E(J_{m,m+1})$	standard deviation $\sqrt{D(J_{m,m+1})}$	skewness α_3	kurtosis α_4	coefficient of variation c
0.02 r_0	0.998 J_0	0.002 J_0	-2.796	11.512	0.002
0.06 r_0	0.987 J_0	0.018 J_0	-2.627	9.781	0.019
0.10 r_0	0.965 J_0	0.047 J_0	-2.356	7.344	0.049
0.14 r_0	0.935 J_0	0.083 J_0	-2.056	5.080	0.089
0.18 r_0	0.899 J_0	0.121 J_0	-1.769	3.295	0.134
0.22 r_0	0.861 J_0	0.158 J_0	-1.511	1.974	0.183
0.26 r_0	0.821 J_0	0.192 J_0	-1.284	1.015	0.234
0.30 r_0	0.781 J_0	0.222 J_0	-1.086	0.317	0.284

TABLE III

EXPECTED VALUE, STANDARD DEVIATION, SKEWNESS, KURTOSIS AND COEFFICIENT OF VARIATION FOR THE NEAREST NEIGHBOUR TRANSFER INTEGRAL $J_{m,m+1}$ DISTRIBUTIONS FOR UNCORRELATED GAUSSIAN FLUCTUATIONS IN MOLECULAR POSITIONS δz_m – FLUCTUATIONS OCCUR ONLY IN PERPENDICULAR DIRECTION TO THE RING PLANE (EIGHT STRENGTHS Δ_z)

Non–Gaussian distributions of $J_{m,m+1}$ manifest themselves by nonzero skewness and kurtosis in all four cases of static disorder connected with deviations in ring geometry. Skewness is negative for static disorder δr_m in radial positions of molecules and static disorder δz_m in molecular positions in perpendicular direction to the ring plane. Contrary, in case of static disorder $\delta \nu_m$ in angular positions of molecules and static disorder $\delta \vec{r}_m$ in molecular positions in arbitrary direction the distribution of $J_{m,m+1}$ is skewed to the right hand side. Most significant skewness can be seen in fourth type of static disorder – fluctuations $\delta \vec{r}_m$ of molecular positions in arbitrary direction (Figure 7 and Table IV).

Due to nonconstant expected value, influences of different types of fluctuations to distribution of $J_{m,m+1}$ can be compared using coefficient of variation. Our previous investigations [35] led to suitable strength of static disorder in transfer integrals $\Delta_J \approx 0.15\ J_0$ and consequently $c \approx 0.15$. As concerns other types of static disorder, approximately same value of coefficient of variation corresponds to the following disorder strengths: $\Delta_r \approx 0.16\ r_0$, $\Delta_\nu \approx 0.012\pi$, $\Delta_z \approx 0.20\ r_0$ and $\Delta_\rho \approx 0.09\ r_0$.

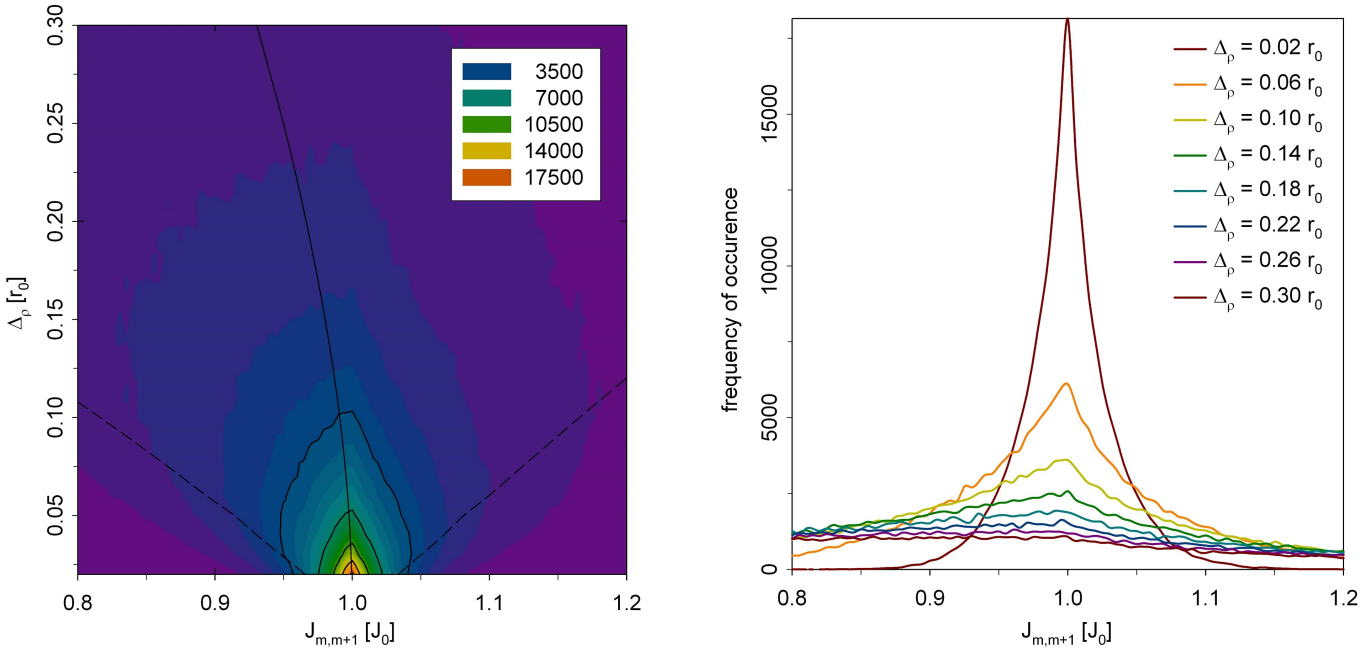

Fig. 7. Distributions of the nearest neighbour transfer integrals $J_{m,m+1}$ for B850 ring from LH2 complex – uncorrelated fluctuations $\delta\vec{r}_m$ of molecular positions in arbitrary direction (Gaussian distribution and standard deviation Δ_ρ, strengths of static disorder $\Delta_\rho \in \langle 0.02\ r_0, 0.30\ r_0 \rangle$)

Δ_ρ	expected value $E(J_{m,m+1})$	standard deviation $\sqrt{D(J_{m,m+1})}$	skewness α_3	kurtosis α_4	coefficient of variation c
0.02 r_0	0.999 J_0	0.034 J_0	0.224	1.959	0.034
0.06 r_0	0.997 J_0	0.103 J_0	0.694	2.953	0.103
0.10 r_0	0.991 J_0	0.175 J_0	1.248	5.644	0.176
0.14 r_0	0.983 J_0	0.252 J_0	2.021	13.038	0.257
0.18 r_0	0.972 J_0	0.341 J_0	3.473	43.644	0.351
0.22 r_0	0.960 J_0	0.453 J_0	7.192	216.533	0.472
0.26 r_0	0.946 J_0	0.607 J_0	16.872	1122.938	0.642
0.30 r_0	0.931 J_0	0.963 J_0	53.337	7706.209	1.034

TABLE IV
EXPECTED VALUE, STANDARD DEVIATION, SKEWNESS, KURTOSIS AND COEFFICIENT OF VARIATION FOR THE NEAREST NEIGHBOUR TRANSFER INTEGRAL $J_{m,m+1}$ DISTRIBUTIONS FOR UNCORRELATED GAUSSIAN FLUCTUATIONS $\delta\vec{r}_m$ OF MOLECULAR POSITIONS IN ARBITRARY DIRECTION (EIGHT STRENGTHS Δ_ρ)

V. CONCLUSIONS

Comparison of the results obtained within different types of static disorder connected with fluctuations in molecular positions can be summarized as follows. Expected value of the nearest neighbour transfer integral distribution depends on static disorder strength for all presented types of fluctuations. The most essential change appears in case of static disorder in radial positions of molecules and static disorder in molecular positions in perpendicular direction to the ring plane. The dependence of standard deviation of the nearest neighbour transfer integral distribution on the static disorder strength shows the highest nonlinearity in case of static disorder in positions of molecules in arbitrary direction. This is connected with the highest skewness and kurtosis of this distribution. It leads to elimination of static disorder strength higher then $0.15\ r_0$ for this type of static disorder. Through the comparison of coefficient of variation we are able to estimate suitable strength of static disorder types connected with fluctuations in molecular positions.

REFERENCES

[1] D. W. Lawlor, *Photosynthesis*, Spriger, New York 2001.
[2] R. van Grondelle and V. I. Novoderezhkin, Energy transfer in photosynthesis: experimental insights and quantitative models, *Phys. Chem. Chem. Phys.* 8, 2003, pp. 793–807.

[3] G. McDermott, et al., Crystal structure of an integral membrane light-harvesting complex from photosynthetic bacteria, *Nature* 374, 1995, pp. 517–521.
[4] M. Z. Papiz, et al., The structure and thermal motion of the B 800-B850 LH2 complex from Rps. acidophila at 2.0 A resolution and 100 K: new structural features and functionally relevant motions, *J. Mol. Biol.* 326, 2003, pp. 1523–1538.
[5] W. P. F. de Ruijter, et al., Observation of the Energy–Level Structure of the Low–Light Adapted B800 LH4 Complex by Single–Molecule Spectroscopy, *Biophys. J.* 87, 2004, pp. 3413–3420.
[6] R. Kumble and R. Hochstrasser, Disorder–induced exciton scattering in the light–harvesting systems of purple bacteria: Influence on the anisotropy of emission and band $\rightarrow$ band transitions, *J. Chem. Phys.* 109, 1998, pp. 855–865.
[7] V. Nagarajan, et al., Femtosecond pump–probe spectroscopy of the B850 antenna complex of Rhodobacter sphaeroides at room temperature, *J. Phys. Chem. B* 103, 1999, pp. 2297–2309.
[8] V. Nagarajan and W. W. Parson, Femtosecond fluorescence depletion anisotropy: Application to the B850 antenna complex of Rhodobacter sphaeroides, *J. Phys. Chem. B* 104, 2000, pp. 4010–4013.
[9] V. Čápek, I. Barvík and P. Heřman, Towards proper parametrization in the exciton transfer and relaxation problem: dimer, *Chem. Phys.* 270, 2001, pp. 141–156.
[10] P. Heřman and I. Barvík, Towards proper parametrization in the exciton transfer and relaxation problem. II. Trimer, *Chem. Phys.* 274, 2001, pp. 199–217.
[11] P. Heřman, I. Barvík and M. Urbanec, Energy relaxation and transfer in excitonic trimer, *J. Lumin.* 108, 2004, pp. 85–89.
[12] P. Heřman, et al., Exciton scattering in light–harvesting systems of purple bacteria, *J. Lumin.* 94–95, 2001, pp. 447–450.
[13] P. Heřman and I. Barvík, Non–Markovian effects in the anisotropy of emission in the ring antenna subunits of purple bacteria photosynthetic systems, *Czech. J. Phys.* 53, 2003, pp. 579–605.
[14] P. Heřman, et al., Influence of static and dynamic disorder on the anisotropy of emission in the ring antenna subunits of purple bacteria photosynthetic systems, *Chem. Phys.* 275, 2002, pp. 1–13.
[15] P. Heřman and I. Barvík, Temperature dependence of the anisotropy of fluorescence in ring molecular systems, *J. Lumin.* 122–123, 2007, pp. 558–561.
[16] P. Heřman, D. Zapletal and I. Barvík, Computer simulation of the anisotropy of fluorescence in ring molecular systems: Influence of disorder and ellipticity, *Proc. IEEE 12th Int. Conf. on Computational Science and Engineering*, Vancouver: IEEE Comp. Soc., 2009, pp. 437–442.
[17] P. Heřman and I. Barvík, Coherence effects in ring molecular systems, *Phys. Stat. Sol. C* 3, 2006, 3408–3413.
[18] P. Heřman, D. Zapletal and I. Barvík, The anisotropy of fluorescence in ring units III: Tangential versus radial dipole arrangement, *J. Lumin.* 128, 2008, pp. 768–770.
[19] P. Heřman, I. Barvík and D. Zapletal, Computer simulation of the anisotropy of fluorescence in ring molecular systems: Tangential vs. radial dipole arrangement, *Lecture Notes in Computer Science* 5101, 2008, pp. 661–670.
[20] P. Heřman, D. Zapletal and I. Barvík, Lost of coherence due to disorder in molecular rings, *Phys. Stat. Sol. C* 6, 2009, pp. 89–92.
[21] P. Heřman, D. Zapletal and J. Šlégr, Comparison of emission spectra of single LH2 complex for different types of disorder, *Phys. Proc.* 13, 2011, pp. 14–17.
[22] D. Zapletal and P. Heřman, Simulation of molecular ring emission spectra: localization of exciton states and dynamics, *Int. J. Math. Comp. Sim.* 6, 2012, pp. 144–152.
[23] M. Horák, P. Heřman and D. Zapletal, Simulation of molecular ring emission spectra – LH4 complex: localization of exciton states and dynamics, *Int. J. Math. Comp. Sim.* 7, 2013, pp. 85–93.
[24] P. Heřman and D. Zapletal, Intermolecular coupling fluctuation effect on absorption and emission spectra for LH4 ring, *Int. J. Math. Comp. Sim.* 7, 2013, pp. 249–257.
[25] M. Horák, P. Heřman and D. Zapletal, Modeling of emission spectra for molecular rings – LH2, LH4 complexes, *Phys. Proc.* 44, 2013, pp. 10–18.
[26] P. Heřman, D. Zapletal and M. Horák, Emission spectra of LH2 complex: full Hamiltonian model, *Eur. Phys. J. B* 86, 2013, art. no. 215.
[27] P. Heřman and D. Zapletal, Emission Spectra of LH4 Complex: Full Hamiltonian Model, *Int. J. Math. Comp. Sim.* 7, 2013, pp. 448–455.
[28] P. Heřman and D. Zapletal, Simulation of Emission Spectra for LH4 Ring: Intermolecular Coupling Fluctuation Effect, *Int. J. Math. Comp. Sim.* 8, 2014, pp. 73–81.
[29] D. Zapletal and P. Heřman, Photosynthetic complex LH2 – Absorption and steady state fluorescence spectra, *Energy* 77, 2014, pp. 212–219.
[30] P. Heřman and D. Zapletal, Simulations of emission spectra for LH4 Ring – Fluctuations in radial positions of molecules, *Int. J. Biol. Biomed. Eng.* 9, 2015, pp. 65–74.
[31] P. Heřman and D. Zapletal, Computer simulation of emission and absorption spectra for LH2 ring, *LNEE* 343, 2015, pp. 221–234.
[32] P. Heřman and D. Zapletal, Modeling of Absorption and Steady State Fluorescence Spectra of Full LH2 Complex (B850 – B800 Ring), *Int. J. Math. Mod. Meth. Appl. Sci.* 9, 2015, pp. 614–623.
[33] P. Heřman and D. Zapletal, Modeling of Emission and Absorption Spectra of LH2 Complex (B850 and B800 Ring) – Full Hamiltonian Model, *Int. J. Math. Comp. Sim.* 10, 2016, pp. 208–217.
[34] P. Heřman and D. Zapletal, B–α/B–β Ring from Photosynthetic Complex LH4, Modeling of Absorption and Fluorescence Spectra, *Int. J. Math. Comp. Sim.* 10, 2016, pp. 332–344.
[35] P. Heřman, I. Barvík and D. Zapletal, Energetic disorder and exciton states of individual molecular rings, *J. Lumin.* 119–120, 2006, pp. 496–503.
[36] C. Hofmann, T. J. Aartsma and J. Kőhler, Energetic disorder and the B850–exciton states of individual light–harvesting 2 complexes from Rhodopseudomonas acidophila, *Chem. Phys. Lett.* 395, 2004, pp. 373–378.